COMPUTER MODELING OF HIGH-EFFICIENCY SOLAR CELLS*

R. J. Schwartz and M. S. Lundstrom
Purdue University
Lafayette, Indiana

ABSTRACT

Transport equations which describe the flow of holes and electrons in the heavily doped regions of a solar cell are presented in a form that is suitable for device modeling. Two experimentally determinable parameters, the effective bandgap shrinkage and the effective asymmetry factor are required to completely model the cell in these regions. Nevertheless, a knowledge of only the effective bandgap shrinkage is sufficient to model the terminal characteristics of the cell. The results of computer simulations of the effects of heavy doping are presented. The insensitivity of the terminal characteristics to the choice of effective asymmetry factor is shown along with the sensitivity of the electric field and quasi-electric fields to this parameter. The dependence of the terminal characteristics on the effective bandgap shrinkage is also presented.

INTRODUCTION

The need for accurate modeling of the physical phenomenon which control the behavior of solar cells has long been recognized as being necessary to the development of high-efficiency solar cells. This paper is concerned with the accurate modeling of heavy doping effects and the proper technique for incorporating experimentally determined heavy doping parameters into a numerical solar cell model.

Since both the emitter and the high-low junction regions of a high-efficiency solar cell are heavily doped, the performance of these regions is controlled by the various heavy doping effects which occur. Among the considerations for correct modeling of these regions are: 1) the regions are degenerate and, therefore, require the use of Fermi-Dirac statistics, 2) the density-of-states function is expected to have a change of shape due to band tailing or the formation of an impurity band, 3) the original energy states are expected to be shifted in energy due to free carrier-ionized impurity interactions, and correlation effects. Recent papers have presented theoretical calculations of the magnitude of these various phenomenon, references 1 to 3. The problem, however, is that the present state-of-the

*This work was supported by the United States Department of Energy through Sandia National Laboratories, contract number 13-2304.

theory is not sufficiently developed. For example, the shape of the density-of-states functions is unknown, and without this information one is unable to compute the parameters which appear in the formulation of the transport equations in the presence of heavy doping effects.

NOTATION

γ	effective asymmetry factor
E_G	bandgap
ΔE_G	bandgap shrinkage
Δ_G	effective bandgap shrinkage
D_p, D_n	hole (electron) diffusion coefficient
$\vec{J}_p, \vec{J}_n$	hole (electron) current density
k	Boltzmann's constant
n_{io}	intrinsic carrier concentration in a semiconductor with an unperturbed band structure
n_{ie}	effective intrinsic carrier concentration
p,n	hole (electron) carrier concentration
q	magnitude of the electronic charge
T	absolute temperature (Kelvin)
V	electrostatic potential
μ_p, μ_n	hole (electron) mobility
X	electron affinity
$\nabla^{\eta_v}, \nabla^{\eta_c}$	The gradient operator with η_v (η_c) held constant

Equilibrium values of the parameters listed above are denoted by a superscript o.

TRANSPORT EQUATIONS

If the existence of a mobility edge separating localized from delocalized states is postulated, transport equations for materials with a position-dependent band structure can be written. These equations in the form given by Marshak and van Vliet (refs. 4, 5) are:

$$J_p = -pq\mu_p \left[\nabla\left(V + \frac{\chi + E_G}{q} - \frac{\Gamma_p}{q}\right)\right] - qD_p\nabla_p \tag{1}$$

$$J_n = -nq\mu_n \left[\nabla\left(V + \frac{\chi}{q} + \frac{\Gamma_n}{q}\right)\right] + qD_n\nabla_n \tag{2}$$

where

$$D_p = \frac{kT}{q}\frac{p}{\frac{\partial n}{\partial \eta_c}}\mu_p \tag{3}$$

and

$$D_n = \frac{kT}{q}\frac{p}{\frac{\partial n}{\partial \eta_c}}\mu_n \tag{4}$$

are the Einstein relations, and

$$\nabla\Gamma_p = \frac{kT}{\frac{\partial p}{\partial \eta_v}}\nabla^{\eta_c}{}_n \tag{5}$$

$$\nabla\Gamma_n = \frac{kT}{\frac{\partial n}{\partial \eta_c}}\nabla^{\eta_c}{}_n \tag{6}$$

are the density-of-states effects.

Without a knowledge of the shape of the density-of-state function and the location of the band edges these equations cannot be utilized for device modeling. Others have formulated transport equations under more restrictive assumptions, such as the rigid band approximation (ref. 6) or under conditions for which Boltzmann statistics apply, (ref. 7). While these formulations allow one to perform numerical calculations, they are restricted to cases which are known to be violated in the emitter and the back surface field region of high efficiency solar cells.

A recent reformulation of the transport equation by Lundstrom, Schwartz and Gray (refs. 8, 9) provides a means of avoiding these complications while retaining a precise model of the effects of heavy doping on the transport equations, and consequently upon the behavior of a solar cell (refs. 8, 9). They have shown that equations 1 and 2 can be rewritten as

$$J_p = -pq\mu_p \left[\nabla\left(V-(1-\gamma)\frac{\Delta_G}{q}\right) \right] - kT\mu_p \nabla_p, \tag{7}$$

and

$$J_n = -nq\mu_n \left[\nabla\left(V + \frac{\gamma\Delta_G}{q}\right) \right] + kT\mu_n \nabla_n, \tag{8}$$

where

$$\Delta_G = (\Delta E_G + \Theta_n + \Theta_p) \tag{9}$$

is the effective bandgap shrinkage and

$$\gamma = \frac{\Delta\chi + \Theta_n}{\Delta_G} \tag{10}$$

is the effective asymmetry factor.

The parameters, θ_n and θ_p, which contain the information on the position dependence of the density-of-states and the influence of Fermi-Dirac statistics are defined by,

$$\nabla\Theta_p = \nabla\Gamma_p - kT\left[\frac{qD_p - kT\mu_p}{p\mu_p}\right] \tag{11}$$

and

$$\nabla\Theta_n = \nabla\Gamma_n - \left[\frac{qD_n - kT\mu_n}{n\mu_n}\right] \tag{12}$$

The significance of recasting the Marshak and van Vliet equations in the form shown by equations (7) and (8) is that the parameters which appear in equations (7) and (8), namely Δ_G and γ, are experimentally determinable. These experimentally determinable parameters contain the information on the band structure and the influence of Fermi-Dirac statistics necessary to model heavily doped semiconductor devices. In addition, the simple, Boltzmann-like form of these equations facilitates their use in device modeling.

The effective gap shrinkage, Δ_G, is the parameter inferred from typical, electrical measurements of heavy doping effects (refs. 10 to 12). Although this parameter is frequently referred to as the bandgap shrinkage, equation 9 shows that Δ_G also accounts for the modified density-of-states and the influence of Fermi-Dirac statistics. The effective gap shrinkage can be related to the effective intrinsic carrier concentration as (refs 8, 9).

$$n_{ie}^2 = n_{io}^2 e^{\Delta G^o/kT} , \tag{13}$$

where n_{io} is the intrinsic carrier concentration for a material with unperturbed band structure.

The parameter γ, which we refer to as the effective asymmetry factor, accounts for the asymmetry in the shift of the band edges as well as the modified density-of-states and the influence of Fermi-Dirac statistics. Like Δ_G, γ can be determined from electrical measurements, but unlike Δ_G, no measurements of γ have been reported.

Equations (7) and (8) can be used by the semiconductor device modeler to account for the complicated effects associated with heavy impurity doping. Unfortunately, information on Δ_G is quite limited, and no information on γ exists. Fortunately, the terminal characteristics of the device are insensitive to γ when the heavily doped regions are in low injection, quasi-neutral, and the dopants fully ionized, (refs. 8, 9). While it is true that the terminal characteristics of the device are unaffected by the choice of γ, it is not true for some of the internal parameters of the cell. For example, the built-in potential, electric field and quasi-electric fields are strongly affected by γ.

The remainder of this paper is devoted to showing the results of computer simulations of solar cells to illustrate the use of the heavy doping model described above. The sensitivity of solar cell performance to the two heavy doping parameters, γ and Δ_G is considered.

SENSITIVITY OF SOLAR CELL PERFORMANCE TO γ

A set of computer simulations was performed in order to test the sensitivity of the device model to the choice of the effective asymmetry factor.* For these simulations, a p^+nn^+ solar cell, described by the parameters listed in Table I, was chosen. The doping profile of the p-n junction in

*The numerical model used for these simulations is described in reference 9.

this device is shown in figure 1. Complete ionization of the impurities was assumed in all simulations. Two different choices for γ were considered. In Case I, we set $\gamma = 0.5$, and in Case II we put all of the effective band edge shift into the majoirty carrier band (i.e. $\gamma = 0$ for p-type, $\gamma = 1$ for n-type). Comparison of the computed, one sun IV curves, shown in Table II, shows that the terminal characteristics of the cell are relatively unaffected by the choice for γ. Similar agreement was observed when the spectral responses for the two cases were compared..

The comparisons of the computed I-V curves for the two cases confirms the prediction (refs. 9, 10) that the terminal characteristics of typical heavily doped semiconductor devices are not sensitive to the choice for γ. Figure 2, however, which compares the open-circuit electric fields within the p-n junction region for the two cases, shows that the electric field is quite sensitive to the choice of γ. The quasi-electric fields for holes and electrons are shown in figure 3. The two choices of γ are seen to result in very different quasi-electric fields, nevertheless, the effective fields which act on the carriers are not affected by γ. The effective fields are the sums of the electric and quasi-electric fields for each carrier. Figures 2 and 3 show that the effective fields for holes and electrons are nearly identical for the two cases.

The open-circuit carrier concentrations within the p-n junction region are plotted in figure 4. As expected, (refs. 8, 9) the carrier concentrations are not sensitive to the choice of γ. Since both the effective fields and carrier concentrations are independent of γ, the current densities are also expected to be unaffected by γ. Figure 5 shows that the expected result is observed.

SENSITIVITY OF SOLAR CELL PERFORMANCE TO Δ_G

The solar cell simulations showed that the terminal IV characteristics of typical silicon solar cells are, as expected (refs. 9, 10) not sensitive to the choice of γ. The performance of silicon solar cells, however, is quite sensitive to the effective bandgap shrinkage, Δ_G. In order to study the effect of Δ_G, we compared the simulated performance of the p^+nn^+ solar cell with the simulated performance of an identical cell in which bandgap narrowing was suppressed (i.e., $\Delta_G = 0$). For these comparisons we chose $\gamma = 0.5$ (all the results to be discussed, however, are independent of the choice of γ).

The computed current versus voltage curves for the p^+nn^+ cell with and without bandgap narrowing are compared in figure 6 which shows the well-known (refs. 13, 14) reduction in open-circuit voltage, V_{OC}, caused by bandgap narrowing. The cause for the reduction in open-circuit voltage can be ascertained by examining figure 7, a plot of the open-circuit energy band diagram for the p-n junction region of the cell. This energy band diagram was computed by employing the rigid band approximation and is for illustrative purposes only. A reduction of the potential barrier for electrons injected into the heavily doped p-type region is shown by figure 7. This reduction of

the potential barrier is caused by Δ_G and it is not affected by γ. The reduced potential barrier results in increased injection of minority carriers into the heavily doped regions which increases the recombination currents associated with these portions of the device and, therefore, reduces the open-circuit voltage.

The computed characteristics of the p^+nn^+ cell, with and without bandgap narrowing, are summarized in Table III. Because this cell was designed (ref. 15) to minimize the deliterious effects associated with heavy impurity doping, the open-circuit voltage of the cell is not severely degraded by bandgap narrowing. In addition, since the short-circuit current of the cell is not significantly affected by bandgap narrowing, the fill factor of the cell is actually improved by bandgap narrowing. This effect, clearly shown by figure 6, minimizes the degradation of cell efficiency caused by bandgap narrowing.

SUMMARY AND CONCLUSIONS

A set of transport equations for use in analyzing heavily doped semiconductor devices has been considered in this paper. The equations were first presented, and the interpretation of the two parameters, Δ_G and γ, used to describe the effects associated with heavy impurity doping was discussed. The influence that these two parameters have on solar cell performance was then illustrated by the results of computer simulation.

The most important conclusion reached in this paper is that heavily doped semiconductor devices can be modeled in terms of two experimentally determinable parameters. The effects associated with heavy impurity doping (i.e., band edge shifts, changes in the density-of-states and the influence of degenerate statistics) can be modeled accurately by using the two parameters in simple, Boltzmann-like transport equations. To model heavily doped semiconductor devices, there is no need to introduce additional, unproven assumptions as is done in the frequently used rigid band approximation. In addition, we have demonstrated that the terminal I-V characteristics of typical, high-efficiency, single-crystal, silicon solar cells are not sensitive to the effective asymmetry factor, γ.

REFERENCES

1. Abram, R. A.; Rees, G. J.; and Wilson, B. L. H.: "Heavily Doped Semiconductors and Devices," Advances in Physics, Vol. 27, pp. 799-892, 1978.

2. Lanyon, H. P. D.; and Tuft, R. A.: "Bandgap Narrowing in Heavily Doped Silicon," IEEE Trans. Electron Devices, Vol. ED-26, pp. 1014-1018, 1979.

3. Mahan, G. D.: "Energy Gap in Si and Ge: Impurity Dependence," J. Appl. Phys., Vol. 51, pp. 2634-2646, 1980.

4. Marshak, A. H.; and van Vliet, K. M.: "Electrical Current in Solids with Position-Dependent Band Structure," Solid-State Electron., Vol. 21, pp. 417-427, 1978.

5. Marshak, A. H.; van Vliet, K. M.: "Carrier Densities and Emitter Efficiency in Degenerate Materials with Position-Dependent Band Structure," Solid-State Electron., Vol. 21, pp. 429-434, 1978.

6. Marshak, A. H.; Shibib, M. A.; Fossum, J. G.; and Lindholm, F. A.: "Rigid Band Analysis of Heavily Doped Semiconductor Devices," IEEE Trans. Electron Devices, submitted for publication.

7. Mock, M. S.: "Transport Equations in Heavily Doped Silicon, and the Current Gain of Bipolar Transistors," Solid-State Electron., Vol. 16, pp. 1251-1259, 1973.

8. Lundstrom, M. S.; Schwartz, R. J.; and Gray, J. L.: "Transport Equations for the Analysis of Heavily Doped Semiconductor Devices," to be published in Solid-State Electron.

9. Lundstrom, M. S.; and Schwartz, R. J.: "Annual Report on Interdigitated Back-Contact Solar Cells, Purdue Univ., School of EE, Tech. Rep., TR-EE 80-14, Jan. 1980.

10. Slotboom, J. W.; and de Graaff, H. C.: "Measurements of Bandgap Narrowing in Si Bipolar Transistors," Solid-State Electron., Vol. 19, pp. 857-862, 1976.

11. van Merbergen, J.; Nijs, J.; Mertens, R.; and van Overstraeten, R.: "Measurement of Bandgap Narrowing and Diffusion Length in Heavily Doped Silicon," in Rec. 13th IEEE Photovoltaic Specialists Conf., 1978.

12. Tang, D. D.: "Heavy Doping Effects in p-n-p Bipolar Transistors," IEEE Trans. Electron Dev., Vol. ED-27, pp. 563-570, 1980.

13. Iles, P. A.; and Soclof, S. I.: "Effect of Impurity Doping Concentration on Solar Cell Output," Conf. Rec., 11th IEEE Photovoltaic Spec. Conf., pp. 19-24, 1975.

14. Godlewski, M. P.; Brandhorst, Jr., H. W.; and Barona, C. R.: "Effects of High Doping Levels on Silicon Solar Cell Performance," Conf. Rec., 11th IEEE Photovoltaic Spec. Conf., pp 32-35, 1975.

15. Fossum, J. G.; Nasby, R. D.; and Burgess, E. L.: "Development of High-Efficiency P^+NN^+ Back-Surface-Field Silicon Solar Cells," Conf. Rec., 13th IEEE Photovoltaic Spec. Conf., pp. 124-129, 1978.

TABLE I PARAMETERS USED TO MODEL THE p^+nn^+ CELL.

Temperature	27°C
Device thickness	300μm
Base doping density	$5 \times 10^{14} cm^{-3}$
PN junction depth	0.35μm
High-Low junction depth	1.0μm
P^+ surface concentration	$1.5 \times 10^{20} cm^{-3}$
N^+ surface concentration	$3.0 \times 10^{20} cm^{-3}$
Doping profiles	complementary error function
SRH lifetime parameter, τ_{po}	400μsec
SRH lifetime parameter, τ_{no}	400μsec
Auger coefficient, A_p	$9.9 \times 10^{-32} cm^6 sec^{-1}$
Auger coefficient, A_n	$2.8 \times 10^{-31} cm^6 sec^{-1}$
Front surface recombination velocity	5000 cm/sec
Back contact	ohmic
Solar spectrum	AM1
Optical reflection losses	0
Bandgap narrowing model (Δ_G)	Slotboom and DeGraaf
Effective asymmetry (γ):	
CASE I	$\gamma = 0.5$
CASE II	$\gamma = 0$ for p-type
	$\gamma = 1$ for n-type

TABLE II. COMPARISON OF 1 SUN I-V CURVES FOR TWO EFFECTIVE ASYMMETRY FACTOR MODELS.

Voltage	Current Density (MA/Cm^2)		Deviation
	Case I	Case II	
0	37.4273	37.4245	7.5×10^{-5}
0.1	37.4259	37.4232	7.2×10^{-5}
0.2	37.4243	37.4216	7.2×10^{-5}
0.3	37.4219	37.4192	7.2×10^{-5}
0.4	37.3932	37.919	3.5×10^{-5}
0.5	36.3423	36.3910	-1.3×10^{-3}
0.6	14.0828	14.9401	-6.1×10^{-2}
0.62	6.1596	4.5492	2.6×10^{-1}

$V_{OC\ Case\ I} = 0.61512$ volts

$V_{OC\ Case\ II} = 0.61632$ volts

TABLE III. COMPARISON OF p^+nn^+ CELL PERFORMANCE WITH AND WITHOUT BANDGAP NARROWING.

	With BGN	Without BGN
Short-Circuit Current	37.43 mA/cm^2	37.59 mA/cm^2
Collection Efficiency	0.98	0.99
Open-Circuit Voltage	0.615 Volts	0.676 Volts
Fill Factor	0.80	0.76
Efficiency	0.192	0.201

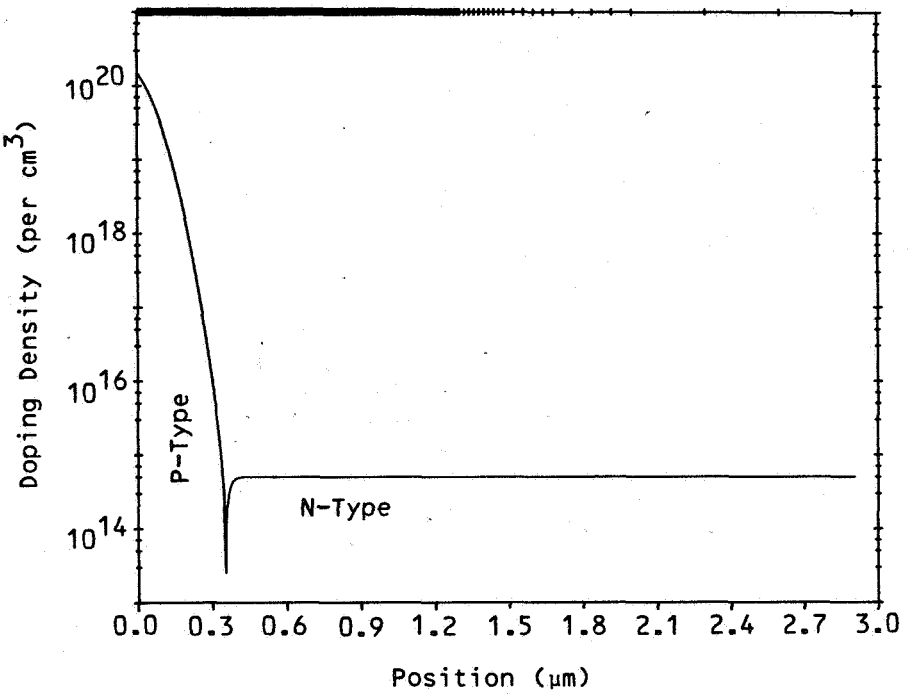

Figure 1. Doping profile for the p-n junction region of the p^+nn^+ solar cell.

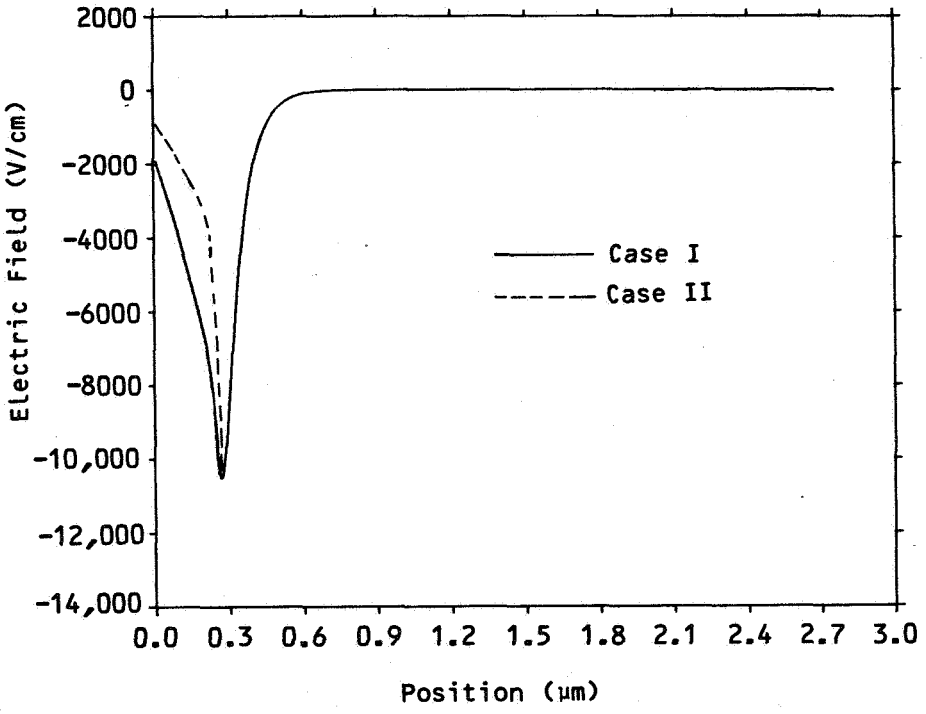

Figure 2. Open-circuit electric field within the p-n junction region of the p^+nn^+ cell.

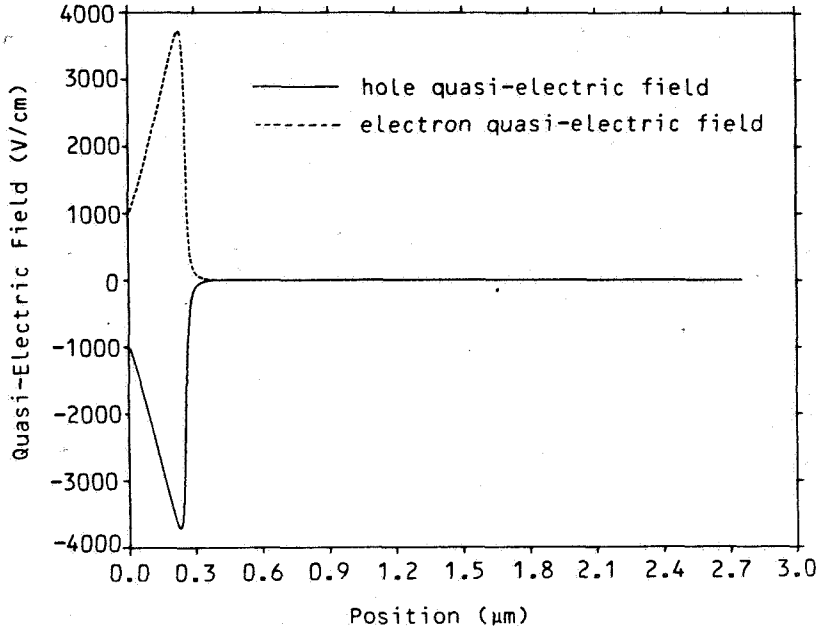

Figure 3a. Quasi-electric fields in the p-n junction region of the p^+nn^+ cell (Case I).

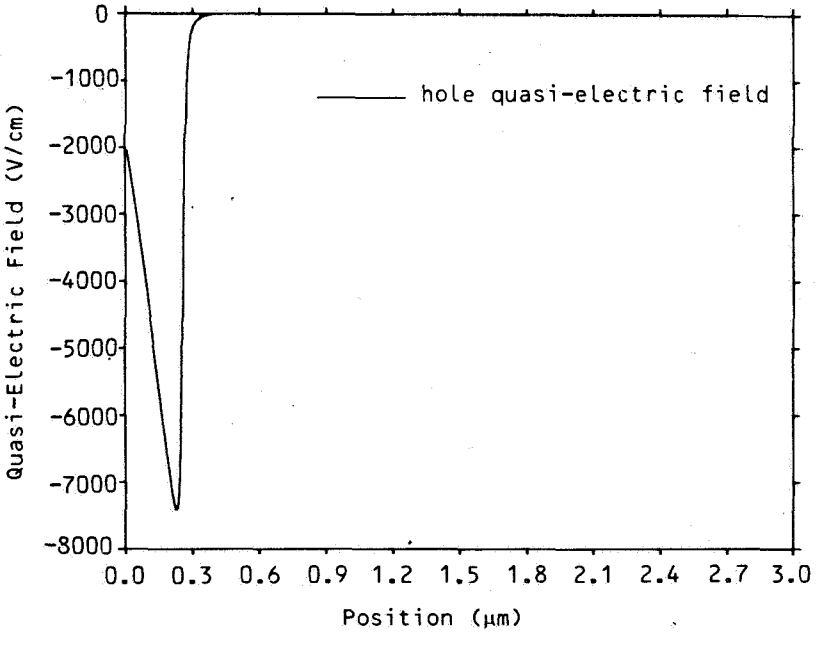

Figure 3b. Quasi-electric field within the p-n junction region of the p^+nn^+ cell (Case II). The electron quasi-electric field is zero for this case.

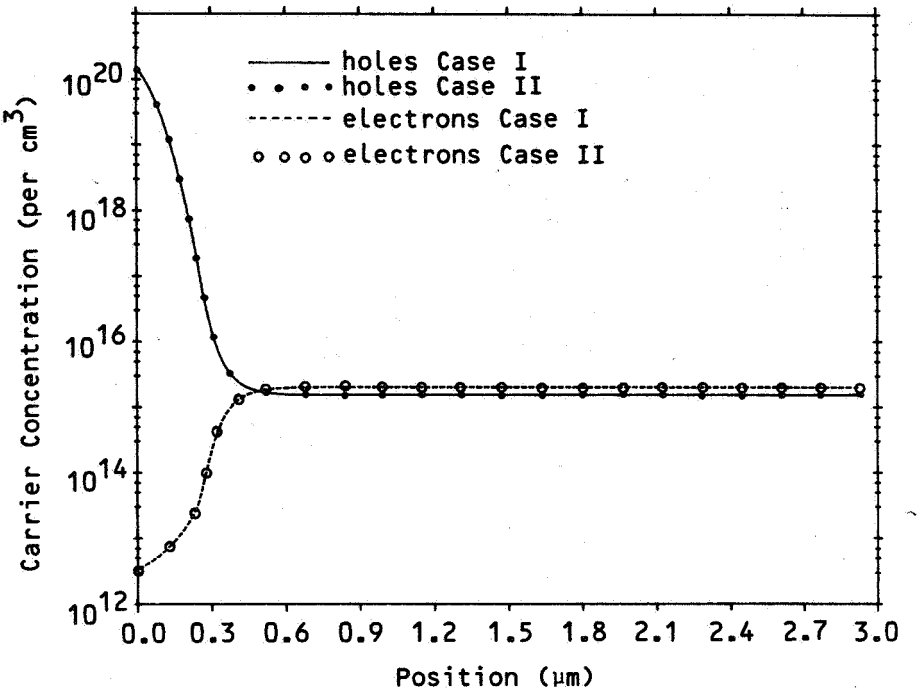

Figure 4. Open-circuit carrier concentrations within the p-n junction region of the p^+nn^+ cell.

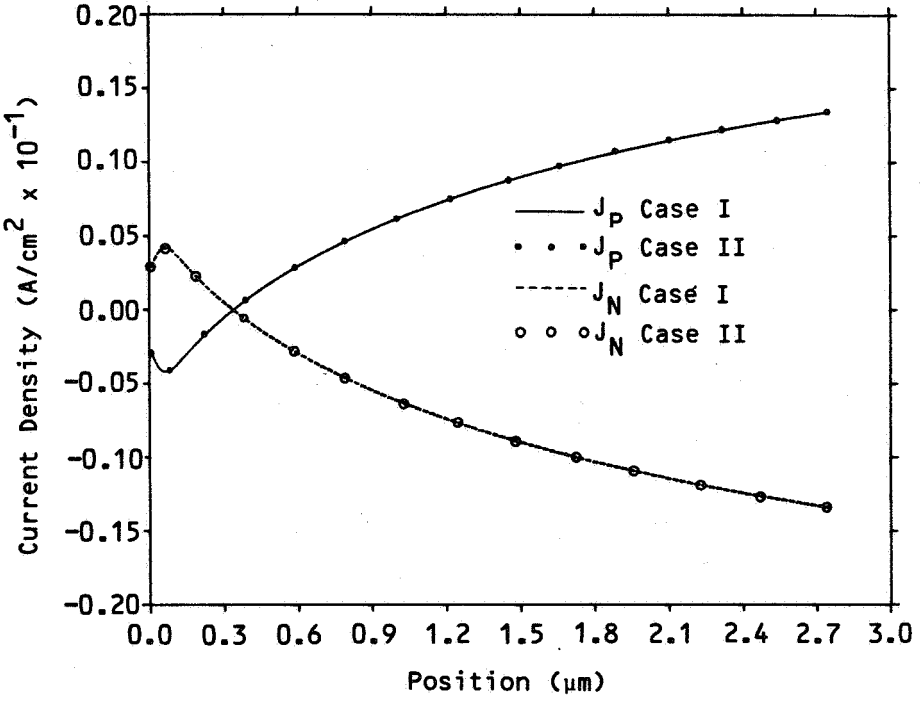

Figure 5. Open-circuit current densities in the p-n junction region of the p^+nn^+ cell.

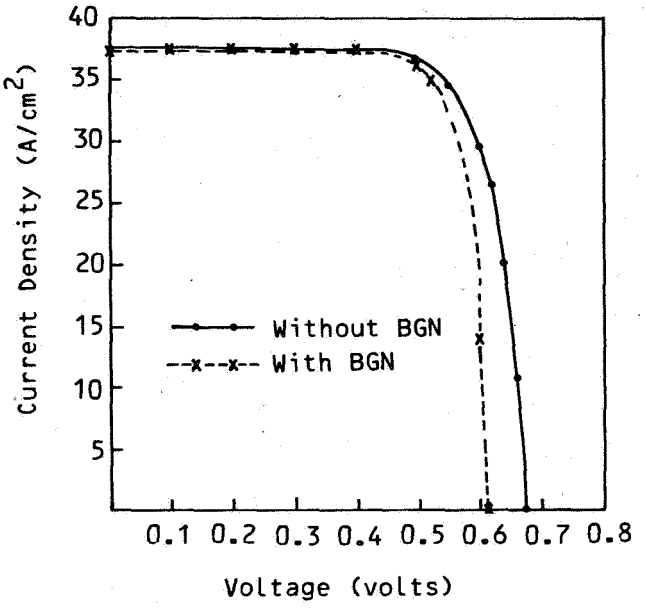

Figure 6. Current-voltage characteristics for a p^+nn^+ solar cell with and without bandgap narrowing.

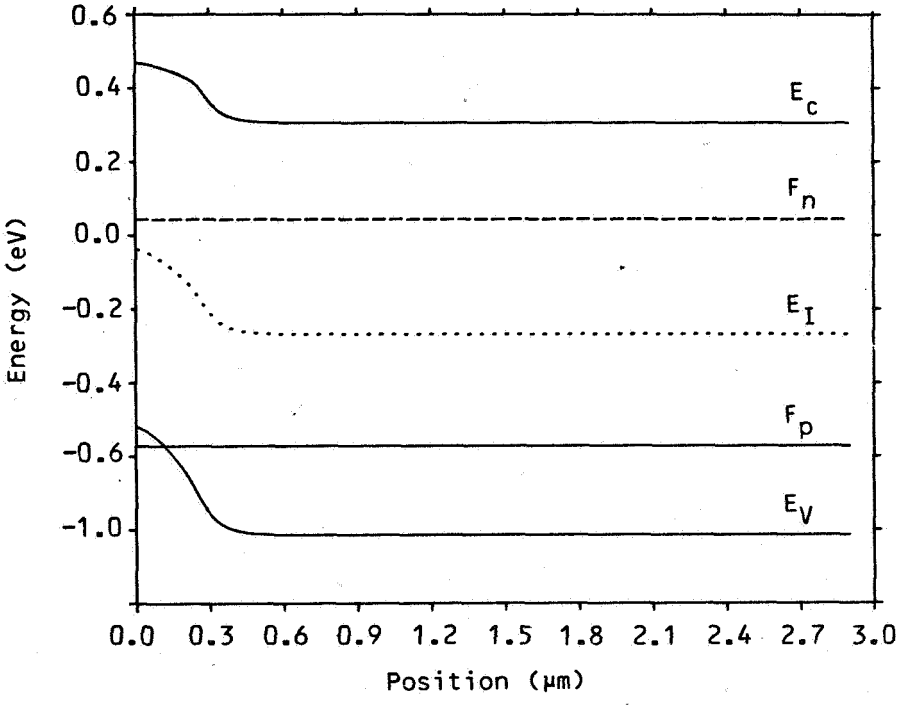

Figure 7. Open-circuit energy band diagram for the p^+nn^+ cell with bandgap narrowing.